DOI: 10.1002/ejic.200800535

The Added Value of Solid-State Pb NMR Spectroscopy to Understand the 3D Structures of Pb Amino Acid Complexes

Laura Gasque,*[a] Michiel A. Verhoeven,[b] Sylvain Bernès,[c] Fabiola Barrios,[a] Jaap G. Haasnoot,[b] and Jan Reedijk[b]

Keywords: Lead / Amino acids / NMR spectroscopy / X-ray diffraction

Single-crystal X-ray diffraction and solid-state ^{207}Pb NMR spectroscopic experiments have been conducted on four lead amino acid complexes with nitrato or perchlorato counterions, namely neutral isoleucine (**1**), deprotonated leucine (**2**), monodeprotonated aspartic acid (**3**), and neutral valine (**4**). The crystal structures reveal that the Pb^{II} ions are preferably coordinated by oxygen atoms and that the amine group of the amino acids is coordinated only in the case of leucine. The results of the solid-state NMR spectroscopic experiments are compared to the 3D structures obtained from single-crystal X-ray data. The NMR spectroscopic experiments show one, two, one, and four lead sites for the Hile, leu$^-$, Hasp$^-$, and Hval complexes, respectively, in agreement with crystal structures. The application of this method towards the characterization of new Pb compounds, for which no 3D structure is known, is discussed and illustrated with an example where a mechanical mixture of two lead complexes is characterized successfully.

Introduction

In spite of the well-documented toxic effects of lead, the detailed molecular mechanisms of its toxic actions remain unknown, and even its coordination chemistry with biomolecules has been scarcely explored. Considered to be an intermediate acid in Pearson's HSAB (Hard and Soft Acids and Bases) classification, Pb^{II} forms very stable complexes with both hard ligands as oxygen donors and soft ligands like sulfur donors; its complexes with oxygen donors are stronger than those of the corresponding calcium complexes, while it also binds more strongly to sulfur donors than the corresponding zinc complexes.[1] However, among the crystal structures deposited in the CSD for Pb^{II} compounds, by far the most common donor atom observed is oxygen, which is present in the coordination sphere of roughly one half of all reported crystal structures, while sulfur is present in less than ten percent of the known Pb^{II}-containing structures.

Recently, there has been an increasing interest in studying the bonding of Pb to natural materials in relation to the study of the ageing processes in old masterpiece paintings, since a substantial amount of the paintings, especially in the Renaissance period, contained lead compounds and were prepared with egg tempera. A typical egg tempera paint is made by grinding egg yolk and water with inorganic pigments like, for instance, lead white [hydrocerussite, $2PbCO_3{\cdot}Pb(OH)_2$], red lead (minium, $2PbO{\cdot}PbO_2$), or red and yellow modifications of litharge (PbO). Recent research has demonstrated that, during the ageing of paint, parts of the binding medium degenerate to small charged organic molecules that undergo new interactions with the pigments and reinforce the paint structure. The newly formed structures are referred to as ionomeric networks.[2–4] Although these networks have so far only been demonstrated in the case of ageing oil paint components, it is possible that deteriorated protein structures also contribute to these networks in the form of stable amino acid salts.

^{207}Pb NMR spectroscopy is an interesting technique whose utility has not been fully explored; while ^{207}Pb NMR spectroscopic studies have been performed on a relatively small number of lead(II) coordination compounds in solution,[5] ^{207}Pb solid-state NMR spectra were mainly reported for ionic lattices or organometallic Pb^{IV}-containing molecules.[6–8] Pb^{II} complexes display a wide variety of coordination numbers,[9] ranging from 2 to 12, and while coordination numbers 4 and 6 are common, the corresponding geometries are predominantly distorted due to presence of a stereoactive $6s^2$ lone electron pair.

[a] Departamento de Química Inorgánica y Nuclear, Facultad de Química, Universidad Nacional Autónoma de México, México D.F., CP 04510, México
Fax: +52-555-622-3811
E-mail: gasquel@servidor.unam.mx
[b] Leiden Institute of Chemistry, P. O. Box 9502, 2300 RA Leiden, The Netherlands
[c] DEP, Facultad de Ciencias Químicas, UANL, Guerrero y Progreso S/N, Col. Treviño, Monterrey N. L., CP 64570, México
Supporting information for this article is available on the WWW under http://www.eurjic.org/ or from the author.

In this paper, we present the coordination compounds obtained from Pb^{II} and four amino acids, namely isoleucine, leucine, aspartic acid, and valine, together with their ^{207}Pb solid-state NMR spectra. The crystallographically independent lead atoms all have a unique chemical shift in their NMR spectra, which suggests that Pb NMR spectroscopy might be a useful tool in obtaining structural information when no 3D structural data can be obtained otherwise.

Results and Discussion

Preparation of the Crystalline Samples

The four compounds discussed in this paper were isolated from aqueous solutions of the corresponding amino acids and $Pb(NO_3)_2$ or $Pb(ClO_4)_2$. A decrease in pH was observed upon mixing, indicative of coordination. An aqueous solution of NaOH was added dropwise with stirring until just before the first appearance of cloudiness, indicative of the formation of $Pb(OH)_2$. The pH value at which this happened varied slightly among the different amino acids employed. Since the reported aqueous equilibrium constants (acid dissociation and stability constants)[10–14] do not suggest any significant difference in affinity for Pb among these amino acids, we feel that the crystallization of these complexes is mostly ruled by the hydrophobic interactions between ligand molecules, rather than by the strength of the metal–ligand interaction. This has been supported by the impossibility to obtain, in similar conditions, crystals with the less hydrophobic aliphatic amino acids (glycine and alanine), even though the thermodynamic stabilities of the corresponding complexes are similar.

Description of the Crystal Structures

The complexes described in this paper, although all were derived from amino acids and have been prepared in a similar manner, have remarkably different structures, as regards the coordination environment of lead, as well as the overall intermolecular network. All these complexes exhibit what has been referred to as "hemidirected coordination geometries",[15] implying a Pb $6s^2$ stereochemically active lone pair of electrons. Table 1 presents relevant metal–ligand bond lengths and angles for the three new structures.

[Pb(Hile)$_2$(NO$_3$)(H$_2$O)$_2$]NO$_3$ (1)

In the solid state, complex **1** may be unambiguously formulated as a monomeric ionic species. The metal center coordinates to two Hile ligands, which are, as expected, in a zwitterionic form, two water molecules, and one didentate nitrate ion. The structure is completed by a noncoordinating nitrate ion. A characteristic feature of the cationic Pb^{II} complex is that the Hile ligands, both including ammonium functionalities, present significantly different coordination modes (Figure 1). The first one acts as a dissymmetric *O*,*O*′ chelating ligand, with Pb–O bond lengths of 2.374(10) and 2.849(7) Å, while the other is a monodentate ligand, with the noncoordinating O atom situated 3.423(12) Å away from the metal center. Such a nonequivalent coordination mode had been described for valine in the molecular complex $[Pb(Hval)_2(NO_3)_2(H_2O)_2]$,[16] but seems to be unprecedented for ile and Hile coordination chemistry.

In the same way, coordinated water molecules display different bonding strengths, as reflected by Pb–(OH_2) bond lengths, 2.508(11) and 2.890(8) Å. Finally one η_2-nitrate ion

Table 1. Selected bond lengths for complexes **1**, **2**, **3**, and **4**.

[Pb(Hile)$_2$(NO$_3$)(H$_2$O)$_2$]NO$_3$ (**1**) Bond lengths [Å]			
Pb1–O1	2.374(10)	Pb1–O2	2.849(7)
Pb1–O3	2.508(11)	Pb1–O4	2.890(8)
Pb1–O11	2.487(9)	Pb1–O21	2.804(10)
Pb1–O22	2.824(12)		

[Pb(leu)(NO$_3$)] (**2**) Bond lengths [Å]			
Molecule 1		Molecule 2	
Pb1–N1	2.420(6)	Pb1′–N1′	2.423(6)
Pb1–O1	2.419(6)	Pb1′–O1′	2.410(6)
Pb1–O1#1	2.590(6)	Pb1′–O1′#3	2.582(7)
Pb1–O2#1	2.775(6)	Pb1′–O2′#3	2.772(6)
Pb1–O3	2.693(11)	Pb1′–O3′	2.699(11)
Pb1–O3#2	2.772(11)	Pb1′–O3′#2	2.768(11)
Pb1–O4#2	2.845(9)	Pb1′–O5′	2.913(9)

Symmetry transformations used to generate equivalent atoms: #1: $-x + 1/2$, $y + 1/2$, $-z + 1$; #2: x, $y - 1$, z; #3: $-x + 1/2$, $y + 1/2$, $-z$.

[Pb(Hasp)(NO$_3$)] (**3**) Bond lengths [Å] from ref.[30]			
Pb1–O1#1	2.706(12)	Pb1–O1#3	2.743(10)
Pb1–O2#1	2.500(11)	Pb1–O3	2.493(12)
Pb1–O4#2	2.536(12)	Pb1–O5	2.730(17)
Pb1–O5#2	2.730(17)		

Symmetry transformations used to generate equivalent atoms: #1: $-x - 1$, $y - 1/2$, $-z + 3/2$; #2: $x + 1$, y, z; #3: $-x - 1/2$, $-y + 2$, $z + 1/2$.

[Pb$_2$(Hval)$_5$](ClO$_4$)$_4$·2(H$_2$O) (**4**) Bond lengths [Å]			
Pb1–O1	2.73(2)	Pb1–O2	2.631(18)
Pb1–O11	2.681(19)	Pb1–O12	2.552(16)
Pb1–O21	2.43(2)	Pb1–O22	2.839(19)
Pb1–O91#1	2.92(2)		
Pb2–O2	2.550(18)	Pb2–O12	2.725(16)
Pb2–O31	2.502(18)	Pb2–O32	2.551(16)
Pb2–O41	2.92(3)	Pb2–O42	2.35(2)
Pb2–O72	2.876(18)		
Pb3–O51	2.619(19)	Pb3–O52	2.636(17)
Pb3–O61	2.648(19)	Pb3–O62	2.646(18)
Pb3–O71	2.43(2)	Pb3–O72	2.78(2)
Pb4–O22#2	2.840(18)	Pb4–O52	2.491(16)
Pb4–O62	2.618(18)	Pb4–O81	2.448(19)
Pb4–O82	2.582(19)	Pb4–O92	2.31(2)

Symmetry transformations used to generate equivalent atoms: #1: x, y, $z + 1$; #2: x, y, $z - 1$.

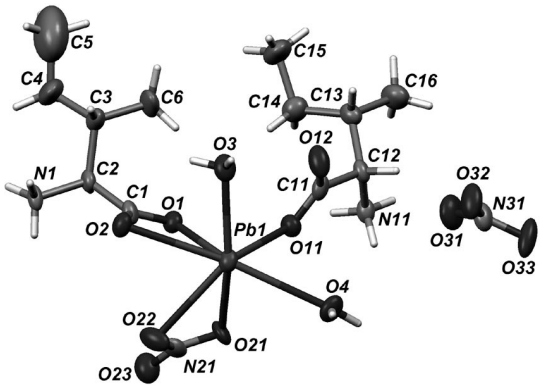

Figure 1. The structure of complex **1**. Displacement ellipsoids for non-H atoms are drawn at the 30% probability level, and the labeling scheme is given for the asymmetric unit.

completes the coordination sphere, resulting in a cationic seven-coordinate Pb^{II} complex. It is worth mentioning that this $[Pb^{II}O_7]$ coordination sphere is not very common; only five X-ray structures are deposited so far in the CSD.[17] On the other hand, regarding the "activity" of the lone pair formally present in the valence shell of Pb^{II},[15] an intermediate situation is also observed for the well-characterized $[PbO_7]$ complexes. Two complexes display holodirected coordination[18,19] spheres, while three are hemidirected.[20–22] Complex **1** is hemidirected, a large void being located almost *trans* to atom O11 belonging to the monodentate Hile ligand (Figure 1).

[Pb(leu)(NO$_3$)] (2)

The asymmetric unit for this compound contains two independent Pb(leu)(NO_3) moieties (Z' = 2) related by a noncrystallographic translation vector oriented along [0 ½ ½]. Both moieties have very similar geometry. The metal center coordinates to a non-zwitterionic L-leucinato ligand, through the amine N and one O carboxylate atom, and to a nitrate ion. Both ligands bridge two symmetry-related Pb^{II} ions, forming a zigzag 1D polymeric framework (Figure 2). Bridging leu^- ligands were previously observed in a polymeric Zn^{II} compound[23] and a dimeric Ni^{II} cation.[24] The combination of space group *C*2 with Z' = 2 is not exceptional[25,26] and generally arises for good reasons. In the case of chiral compounds, such a combination allows two molecules to be related by a noncrystallographic inversion center.[27] This arrangement has been observed for instance in catena-tetra-aqua-(μ_2-L-aspartate-*N*,*O*)-calcium(II).[28] In the case of compound **2**, two polymeric 1D chains run along the short axis [010], one based on Pb1 and symmetry-related metal centers, and the other based on Pb1′ and symmetry-related metal centers. One polymer is related to the other through a noncrystallographic inversion center, and no significant contacts are observed between them. Because of the zigzag arrangement of metal centers in each strand, no significant metal–metal interactions are present in **2**, the shortest separation being 4.70 Å (van der Waals radii for Pb: 2.02 Å). The coordination sphere in **2** is $[PbO_6N]$, formally related to that observed in **1** after substitution of an O donor by a N donor belonging to the nonprotonated amine group of leu^-. The geometry remains hemidirected, and the Pb lone pair is located *trans* to the leu ligand. To date, only one Pb complex with a $[PbO_6N]$ coordination environment, which has been characterized by single-crystal X-ray crystallography, has been reported,[29] although in that case, it is unclear whether the coordination sphere is hemi- or holodirected.

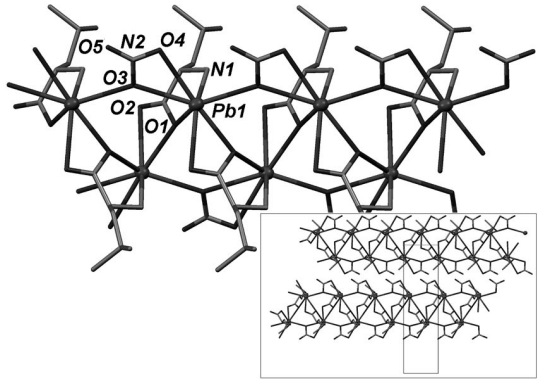

Figure 2. A part of the polymeric structure of **2**. A single chain, corresponding to one independent Pb atom in the asymmetric unit is represented. Labeled atoms belong to the asymmetric unit. The inset represents two crystallographically independent chains running along [010]. The cell is oriented down axis [100]. In both figures, H atoms have been omitted for clarity.

[Pb(Hasp)(NO$_3$)] (3)

The X-ray structure of this complex was previously reported and may be described as a 3D polymeric framework built up by association of [Pb(Hasp)(NO_3)] moieties through bridging carboxylate functionalities of $Hasp^-$ ligands.[30] The metal centers are hemidirected and surrounded by seven donor O atoms from $Hasp^-$ and nitrato ligands (see Figure 3).

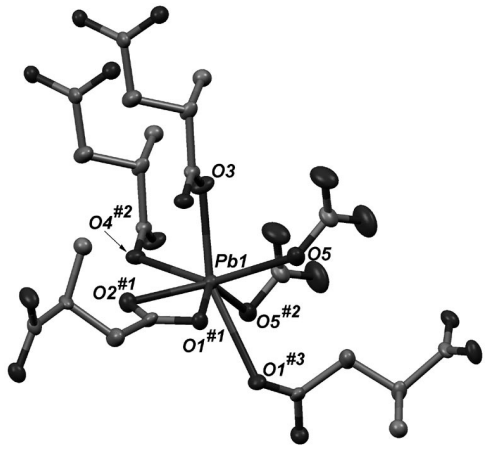

Figure 3. Coordination geometry around the metallic center in the polymeric compound [Pb(Hasp)(NO_3)], **3**. Symmetry codes are given in Table 1. The $6s^2$ lone pair of Pb^{II} is located almost *trans* to O3.

[Pb$_2$(Hval)$_5$](ClO$_4$)$_4$·2(H$_2$O) (4)

The asymmetric unit for complex **4** includes four independent Pb atoms coordinated to ten valine ligands, all in a zwitterionic form, eight free perchlorate ions and four uncoordinated water molecules, giving $[Pb_2(Hval)_5]^{4+}$ as a minimal formula for the complex cation. The whole structure for the complex is a 1D polymer, formed by association of $[Pb_2(Hval)_5]^{4+}$ monomeric species. However, along this polymer, a variety of coordination modes is present for ligands, due to the duplicated $[Pb_2(Hval)_5]^{4+}$ moiety in the asymmetric unit. For the independent set of 10 Hval ligands, 7 are tridentate bridging ligands (μ-Hval-*O*,*O*,*O*′ mode), 2 are didentate nonbridging ligands (Hval-*O*,*O*′ mode), while the last one is a didentate bridging ligand (μ-Hval-*O*,*O*′ mode). The first binding mode seems to be unprecedented in the coordination chemistry of valine to any metal. The last two binding modes have only been described previously for mixed-ligand complexes with valine.[16,31]

Each coordination mode has a specific role in the building of the polymeric structure. μ-Hval-*O*,*O*,*O*′ essentially connects metal centers within the asymmetric unit; the unique μ-HVal-*O*,*O*′ connects asymmetric units; and finally, nonbridging Hval-*O*,*O*′ ligands complete the coordination spheres of two of the four independent Pb atoms.

The resulting structure is a 1D polymer (Figure 4) oriented along cell axis [001]. Contrasting with the arrangement found in polymer **2**, the lack of a zigzag arrangement for the metal centers in **4** precludes metal–metal interactions. Indeed, a sequence of short and long Pb···Pb separations is observed along the polymer. The two short distances, Pb1···Pb2 = 4.0797(18) Å and Pb3···Pb4 = 4.0439(17) Å, actually correspond to van der Waals contacts and alternate with nonbonding separations, Pb2···Pb3 = 4.3853(18) Å and Pb4···Pb1^{i} = 4.3652(18) Å (symmetry code *i*: *x*, *y*, *z* – 1). Chains are packed parallel in the crystal structure, without significant interactions between them. The coordination mode of Pb^{II} ions in **4** may be considered as a mixture of [PbO$_7$] and [PbO$_6$] coordination spheres, in a ratio of 3:1. Regardless of the number of atoms surrounding the metal ions in **4**, the observed geometry is clearly hemidirected, which is consistent with the result obtained for other complexes.

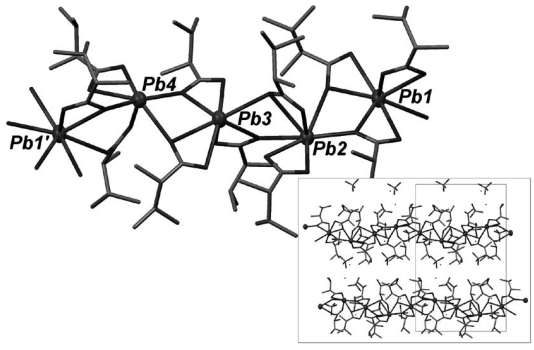

Figure 4. A part of the polymeric structure formed by cations in **4**. The asymmetric unit contains atoms Pb1 to Pb4. Symmetry code for Pb1′: *x*, *y*, *z* – 1. The inset represents a packing diagram including two symmetry-related cationic polymers, and embedded anions and water molecules. The cell is oriented down axis [100]. In both figures, H atoms have been omitted for clarity.

^{207}Pb Solid-State NMR Spectroscopy

The chemical shift in NMR spectroscopy is an anisotropic property that can be described by three independent perpendicular values (i.e. the tensor elements δ_{11}, δ_{22}, δ_{33}). In solid-state ^{207}Pb NMR spectroscopy, the chemical shift anisotropy interaction often exceeds the highest feasible spin rate, which is 12–15 kHz for a 4 mm sample holder. The presented spectra show multiple, evenly spaced resonance peaks that describe the chemical shift envelope. For the sake of comparison, it is convenient to express the anisotropy of the chemical shift in its isotropic value (δ_i), the

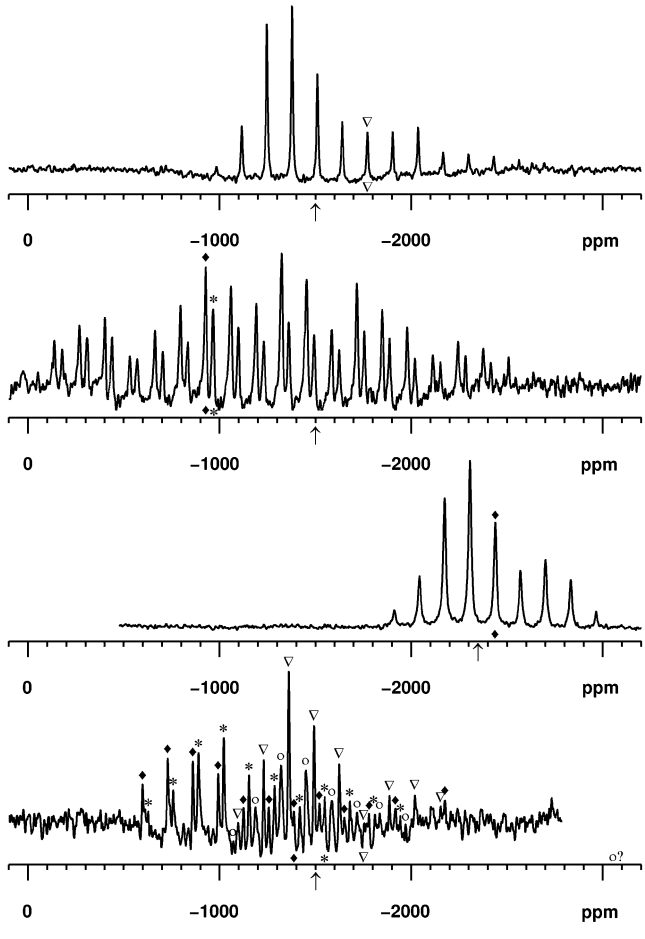

Figure 5. Solid-state ^{207}Pb spectra of the Pb^{2+} complexes of isoleucine, leucine, aspartic acid, and valine (top to bottom). The center band of each signal is indicated with a symbol on the axis. In the bottom spectrum, all resonances are labeled at the top of the peaks to indicate the CS envelope of each lead atom. The transmitter frequency is indicated with a ↑. Labeling symbols as are assigned in Table 2.

Table 2. Summary of the recorded values and derived parameters of solid-state ^{207}Pb NMR spectroscopic experiments on four lead amino acid complexes.

Site[a]		δ_i [ppm]	δ_{11} [ppm]/ *n*th side band	δ_{33} [ppm]/ *n*th side band	calculated δ_{22} [ppm]	span [Hz][b]	δ_{aniso} [ppm][c]	η_{aniso}[c]
Lead(II) Hile site 1	▽	–1774	–1060[d]	–2994[d]	–1268[d]	$\approx 162\times10^3$	-1220 ± 32[d]	0.17 ± 0.09[d]
Lead(II) leu⁻ site 1	♦	–929	121/–8	–2773/+14	–135	$\approx 2.5\times10^5$	$-18\times10^2\pm3\times10^2$	0.14 ± 0.10
site 2	*	–969	84/–8	–2814/+14	–177	$\approx 2.5\times10^5$		
Lead(II) Hasp site 1	♦	–2439	–1969[d]	–3045[d]	–2303[d]	$\approx 90\times10^3$	-606 ± 31[d]	0.55 ± 0.18[d]
Lead(II) Hval site 1	♦	–1390	–600/–6	n.d	n.d	$>1.4\times10^5$	negative	n.d.
site 2	*	–1549	–630/–7	n.d.	n.d.	$>1.5\times10^5$	negative	n.d.
site 3	▽	–1755	–1097/–5	n.d	n.d	$>1.1\times10^5$	negative	n.d.
site 4	o	n.d	–1073/n.d.	n.d.	n.d.	$>>0.4\times10^5$	negative	n.d.

[a] The crystal sites are numbered from downfield to upfield. The symbols refer to the signals in the figures. [b] Estimation of the difference between the outermost resonances at the upfield and downfield edge of the spectrum. [c] Estimation of the shape of the anisotropy of the chemical shift envelope based on the observed δ_{iso}, δ_{11}, and δ_{33}. The parameter δ_{aniso} is defined as $\delta_{zz} - \delta_{iso}$; if the envelope extends more upfield than downfield with respect to δ_{iso}, the value of δ_{aniso} is negative.[32,33,34] [d] Fitted with SIMPSON in combination with MINUIT.[32,35]

anisotropy parameter (δ_{aniso}), and the asymmetry parameter (η) of the chemical shift envelope.[32–34] These parameters can be extracted by fitting to a simulated spectrum. Subsequently, these parameters can be related to structural parameters. Figure 5 shows spectra of the lead amino acid complexes discussed in this work, Table 2 shows the extracted chemical shift parameters.

Detailed Discussion of Solid-State NMR Spectra

[Pb(Hile)$_2$(NO$_3$)(H$_2$O)$_2$]NO$_3$ (1)

The NMR response for [Pb(Hile)$_2$(NO$_3$)(H$_2$O)$_2$]NO$_3$ consists of one well-defined sharp signal. The isotropic chemical shift is found at δ = –1774 ppm. Since the chemical shift envelope is wide and the excitation of resonances more than 75 kHz away from the transmitter offset are attenuated, an additional spectrum with transmitter at –3000 and –500 ppm was recorded to estimate the upfield and downfield edge of spectrum (see Supporting Information). These data were used as initial input for a simulation of the chemical shift anisotropy parameter. The calculated value for the anisotropy is –1220 ppm and the asymmetry 0.17, indicating nearly axial symmetry for the chemical shift tensor.

[Pb(leu)(NO$_3$)] (2)

In the crystal structure of [Pb(leu)(NO$_3$)] two lead sites are present that differ slightly. The crystal is built up of two crystallographically independent parallel 1D coordination polymers that extend along the *b* axis as described above. Two differences between the polymeric 1D chains are highlighted. The first difference is the bridging nitrate anion that is rotated toward one of two adjacent lead atoms. Both polymer chains have an oxygen atom of the nitrate ion that bridges between two adjacent lead atoms, while the other two oxygen atoms of the nitrate ion are weakly coordinating. In one of the parallel chains, the nitrate ion is more tilted towards the positive *b* axis, and in the other chain in the direction of the negative *b* axis (Scheme 1). Interestingly, the overall deviations in bond lengths and angles between lead and the coordination sites of the leucinate and the bridging nitrate oxygen are all smaller than 0.05 Å and 3°, respectively, between the two chains, except for the distances of the weakly coordinating nitrate oxygen atoms which are 3.11/2.85 and 2.91/3.04 Å for the respective chains.

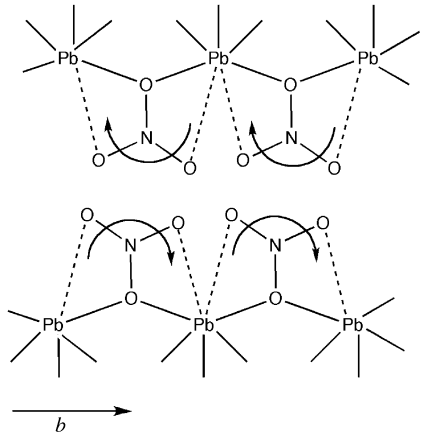

Scheme 1. Schematic representation of the arrangement of the nitrate ions with respect to the lead atom in the nearly identical 1D polymers.

The second difference is the distance in the *ac* plane between a lead atom (Pb1 or Pb1′) and the closest leucine methyl group of the other polymer chain (C1′ or C1, respectively). The distances Pb1–C1′/Pb′–C1 are 5.22 vs. 5.37 Å. These Pb1–C1′ and Pb1′–C1 vectors seem to coincide largely with the position of the 6s^2 pair, which is probably located *trans* to the bisector Pb1–N1/Pb1–O1. These relatively small deviations seem to cause a shift of 40 ppm, –929 vs. –969 ppm, between the two chains. The span of both chemical shift envelopes is estimated to be approxi-

mately 2.5×10^5 Hz, after recording additional spectra for determination of the up- and downfield edges of the signal (see Supporting Information). The envelope is large relative to literature values. On the basis of the observed values of the isotropic chemical shift and edges of the spectrum (δ_{11} and δ_{33}), the anisotropy appears to be not far off axial symmetry ($\eta = 0.14 \pm 0.1$). From the available data, it is unclear how the perpendicular elements of the chemical shift interact mutually; however, computational chemistry on this particular example would be particularly interesting to understand the relation between chemical shift and structure for lead compounds.

[Pb(Hasp)(NO$_3$)] (3)

The crystal structure of [Pb(Hasp)(NO_3)] indicates one unique lead site, also the MAS NMR spectrum shows one well-defined signal that has its center band at δ = –2439 ppm. The signal is shifted significantly upfield relative to the previous two compounds. The chemical shift envelope is relatively modest (90 kHz). The width and anisotropy of the chemical shift envelope have been fitted, resulting in an anisotropy of –606 ppm and an asymmetry of 0.55 (see Table 2/Supporting Information).

[Pb$_2$(Hval)$_5$](ClO$_4$)$_4$·2(H$_2$O)$_2$ (4)

The solid-state NMR response of $[Pb_2(Hval)_5](ClO_4)_4 \cdot 2H_2O$ in polymer **4** shows four discrete signals in accordance with the four independent lead sites in the crystal. Analysis of the resonances at different spinning speeds made it possible to determine three isotropic chemical shifts (see Table 2). The fourth signal is broad or might be a superposition of two resonances and it was not possible to univocally determine the isotropic chemical shift of this signal. Additional experiments at lower spin rate might perhaps give a more definite result. Since it is extremely time-consuming to obtain a sufficient signal-to-noise ratio in the spectral region upfield from –1800 ppm, it was not feasible to determine the extent of the upfield edge of the chemical envelope (δ_{33}) for the Pb sites in this sample. However, the relative signal strength of the spinning side bands upfield and downfield with respect to $\delta_{i''}$ indicates that δ_{aniso} has a negative sign. Although no unambiguous signals can be detected upfield from –1800 ppm, it seems that the fourth signal follows the shape and envelope width of the signal at δ = –1755 ppm. The relatively low signal intensity and abundance of signals in this sample made it impossible to obtain a sufficient signal-to-noise ratio for determination of chemical shift parameters. However, qualitatively the NMR response of the sample shows a similar trend with respect to isotropic chemical shift and envelope width relative to the other amino acid salts. In addition, the data seem to indicate that the Pb sites are pairwise comparable.

Validation of the Method: Use of a Physical Mixture of [Pb(Hile)$_2$(NO$_3$)(H$_2$O)$_2$]NO$_3$ and [Pb(leu)(NO$_3$)]

Solid-state ^{207}Pb NMR spectroscopy has previously been used to characterize physical mixtures of lead halides[36] and mixed lead halides of the type PbXX′, where X and X′ are two different halides.[37] To investigate the strength and possibilities of this method, a mixture of two species was studied. In Figure 6 the spectrum of a mechanical 1:1 mixture of two lead amino acid complexes is presented. The spectrum is recorded with the transmitter frequency at δ = –1250 ppm. The signals of both complexes can be readily distinguished. Between –1000 and –1500, the strong signals of **1** overlap the signal at δ = –969 ppm of compound **2**. Since the NMR response of each lead amino acid complex has such a distinct shape determined by the isotropic chemical shift, the width of the chemical shift envelope of the two components of the mixture can easily be recognized. Indeed, ^{207}Pb NMR spectroscopy can be a very useful method to characterize the components of a mixture of such compounds. It is clear though that the detection of a small amount of a species is hampered by the fact that some signals have a wide chemical shift envelope.

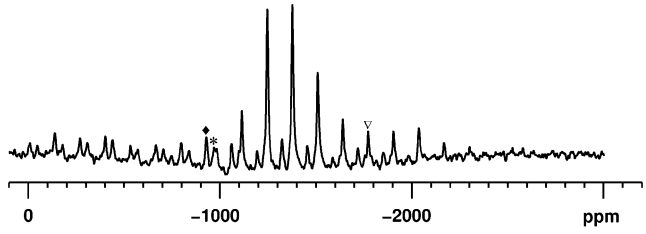

Figure 6. Solid-state ^{207}Pb NMR spectrum of a mechanical 1:1 mixture of Pb(leu)(NO_3), (♦, *) and [Pb(Hile)$_2$(NO_3)(H_2O)$_2$]NO_3 (▽), the center band of each signal is indicated with a symbol.

Conclusions

We have characterized three new Pb^{II} complexes, which, in spite of very different structural features, invariably stabilize a hemidirected geometry around Pb^{II} ions, in line with a stereochemically active lone pair. Thus, assuming that in these zwitterionic amino acids almost all donor atoms are O, coordination numbers of 6 or 7 favor the activity of the Pb^{II} lone pair. However, no far-reaching conclusions should be drawn on the basis of this reduced set of structures. It is well-known that in many Pb^{II} complexes, the lead–donor-atom distances are widely spread, as exemplified in complex **1**. Some arbitrariness may then result in the identification of a donor atom, and in turn, in the correct description of the coordination geometry. Definitely, one should not rely on X-ray structures only for resolving these issues.

The results from measurements of the powder solid-state ^{207}Pb response strongly support the data obtained by X-ray studies on single crystals. There seems to be a tendency of axial symmetric electron distributions around the lead nucleus, as indicated by the low asymmetry parameter (η),

which could be related to the stereochemically active lone pair that is often observed in lead compounds. Since the excitation of the resonances was limited to 75 kHz by the transmitter offset, the NMR signals at the edges have been measured in separate experiments to estimate the principal values of the chemical shift. Comparison of the NMR spectroscopic data with the coordination structure can in some cases reveal a relationship between the CSA parameters and, for instance, the average bond lengths or bond angles. Up till now, no such correlation has been reported in the literature for lead, likely because there are additional geometrical considerations that should be evaluated. Because of the small set of data presented, it is anticipated that a relationship will have to evolve from a detailed analysis of additional NMR spectroscopic data, available crystal structures, and computational chemistry. Finally, our experiments show that solid-state ^{207}Pb NMR spectroscopy can be applied easily to qualitatively describe a mixture of compounds; this might be a useful tool in the future for analysis of salt structures in paintings.

Experimental Section

General: All complexes were isolated from aqueous solutions of analytical grade reactants, prepared with freshly degassed water. Ligand abbreviations: neutral amino acids are represented by Hile, Hleu, Hval, and H_2asp.

[Pb(Hile)$_2$(NO$_3$)(H$_2$O)$_2$]NO$_3$ (1): Lead nitrate (1.65 g, 5 mmol) was dissolved in water (50 mL) and combined with a solution of isoleucine (2.6 g, 10 mmol) in water (50 mL). The pH was adjusted to 4.5 with NaOH (0.1 M), and the solution was left to crystallize. Colorless plates were collected after three days. Yield: 3.1 g (73%). $Pb(C_6H_{13}NO_2)_2(H_2O)_2(NO_3)_2$ (629.59): calcd. C 22.89, H 4.77, N 8.90; found C 23.32, H 4.65, N 8.76.

[Pb(leu)(NO$_3$)] (2): Lead nitrate (1.65 g, 5 mmol) was dissolved in water (50 mL) and combined with a solution of leucine (2.6 g, 10 mmol) in water (50 mL). The pH was adjusted to 5.0 with NaOH (0.1 M), and the solution was left to rest. Colorless prisms suitable for X ray diffraction were collected after several days. Yield: 2.52 g (59%). $Pb(C_6H_{12}NO_2)(NO_3)$ (399.37): calcd. C 18.04, H 3.01, N 7.02; found C 18.21, H 3.12, N 6.95.

[Pb(Hasp)(NO$_3$)] (3): This compound was obtained as described previously.[30]

[Pb$_2$(Hval)$_5$](ClO$_4$)$_4$·2H$_2$O (4): Lead perchlorate trihydrate (4.6 g, 10 mmol) was dissolved in water (50 mL) and combined with a solution of valine (1.17 g, 10 mmol) in water (50 mL). The pH was adjusted to 5.5 with NaOH (0.1 M), and the solution was left to crystallize. Approximately a month later, crystals suitable for X-ray diffraction were collected. Yield: 2.3 g (16%). $Pb_2(C_5H_{11}NO_2)_5(H_2O)_2(ClO_4)_4$ (1433.95): calcd. C 20.93, H 4.12, N 4.88; found C 21.1, H 3.99, N 4.96.

Structure Determinations: Single-crystal X-ray diffraction data for **1**, **2**, and **4** were measured at 298 K, with a Bruker P4 diffractometer by using common procedures[38] and corrections for absorption effects were applied on the basis of ψ-scans with χ close to 90°. The structures were solved and refined by using standard procedures.[39,40] H atoms were placed in idealized positions and refined by using a riding model with fixed isotropic displacement parameters. In the case of **1**, even H atoms of water molecules were placed in idealized positions, while in the case of **4**, they were omitted. For **1**, distance C4–C5 was restrained to 1.54(2) Å. For **4**, the geometry for perchlorate anions as well as bond lengths in *i*Pr groups were regularized using soft restraints, otherwise, the geometry that was obtained for these groups would not make sense. The

Table 3. Crystal data for complexes **1**, **2**, and **4**.

Compound	**1**	**2**	**4**
Empirical formula	$C_{12}H_{30}N_4O_{12}Pb$	$C_6H_{12}N_2O_5Pb$	$C_{25}H_{59}Cl_4N_5O_{28}Pb_2$
Formula weight	629.59	399.37	1433.95
Color, habit	plate, colorless	prism, colorless	irregular, colorless
Crystal size [mm]	0.60 × 0.28 × 0.10	0.44 × 0.20 × 0.08	0.60 × 0.36 × 0.32
Space group	$P\,2_12_12_1$	$C\,2$	$P\,2_1$
a [Å]	5.4557(7)	19.8637(12)	12.075(4)
b [Å]	13.656(2)	5.2297(4)	25.569(9)
c [Å]	30.572(5)	19.6208(16)	15.854(5)
β [°]	–	98.644(4)	90.87(3)
V [Å^3]	2277.7(6)	2015.1(3)	4894(3)
Z	4	8	4
$\rho_{calcd.}$ [g cm^{-3}]	1.836	2.633	1.946
μ [mm^{-1}]	7.468	16.745	7.179
2θ range [°]	4–55	4–55	3–50
Reflections collected	4492	3323	12648
Independent reflections (R_{int})	4069 (0.031)	3066 (0.035)	9090 (0.079)
Transmission factors [min., max.]	0.102, 0.475	0.062, 0.213	0.056, 0.101
Final R indices [$I > 2\sigma(I)$] R_1, wR_2	0.049, 0.117	0.025, 0.061	0.066, 0.162
Final R indices (all data) R_1, wR_2	0.073, 0.136	0.029, 0.063	0.091, 0.181
Goodness-of-fit on F^2	1.037	1.083	1.018
Data/restraints/parameters	4069/1/269	3066/1/254	9090/111/1155
Largest difference peak/hole [e Å^{-3}]	1.09, –2.21	1.16, –1.13	2.06, –1.91

R_{int}, R_1, and wR_2 are defined as follows: $R_{int} = \frac{\Sigma|F_o^2 - \langle F_o^2\rangle|}{\Sigma F_o^2}$; $R_1 = \frac{\Sigma||F_o| - |F_c||}{\Sigma|F_o|}$; $wR_2 = \left[\frac{\Sigma w(F_o^2 - F_o^2)^2}{\Sigma w(F_o^2)^2}\right]^{1/2}$.

refinement of a Flack parameter[41] confirmed the absolute configuration of the enantiopure amino acids. Pertinent crystal data are collected in Table 3, and complete crystallographic information is deposited as a CIF file. Structure factors (CIF format) are available on request.

CCDC-623373, -623374, -623375 contain the supplementary crystallographic data for this paper. These data can be obtained free of charge from The Cambridge Crystallographic Data Centre via www.ccdc.cam.ac.uk/data_request/cif.

Experimental NMR Spectroscopic Procedures: Solid-state ^{207}Pb spectra have been recorded with a Bruker DMX-400 9.4 T spectrometer. To reduce "probe ringing", a rotor-synchronized Hahn-echo experiment was used for data acquisition with n = 1.5 rotor periods prior to and after the refocusing pulse. The ^{207}Pb pulse powers were set to ≈ 75 kHz to achieve a broad irradiation, while TPPM proton decoupling was used at ≈ 30 kHz. For initial excitation, a π/2 lead pulse was applied. All spectra were recorded at 303 K to assure identical conditions of the temperature-dependent chemical shift of the ^{207}Pb nucleus. Spectra were recorded with 300 or 500 kHz spectral width. For each compound the irradiation frequency was initially tuned to –1500 ppm, subsequently the irradiation frequency was tuned to the approximate middle of an initial signal. Spectra were recorded at 11 kHz and at 12 kHz to identify the isotropic chemical shift value. Subsequently, the irradiation frequency was tuned to the observed downfield or upfield edge of the spectrum to obtain a more precise estimation of the chemical shift envelope. Saturated lead nitrate was used as a secondary reference at δ = –2970 ppm with respect to tetramethyllead. The spectra of the Hasp$^-$ and Hile compounds have been fitted by SIMPSON in combination with MINUIT[32,35] to extract the CSA parameters, taking into account the irradiation width of the pulses (see Supporting Information).

Supporting Information (see footnote on the first page of this article): Fit of the chemical shift anisotropy parameters for $[Pb(Hile)_2(NO_3)(H_2O)_2]NO_3$ (**1**). Estimation of the chemical shift anisotropy parameters for $[Pb(leu)(NO_3)]$ (**2**). Fit of the chemical shift anisotropy parameters for $[Pb(Hasp)(NO_3)]$ (**3**). SIMPSON input file.

Acknowledgments

M. A. V. thanks E. Daviso for fruitful discussions regarding the SIMPSON script. S. B. is grateful to BUAP for diffraction time. This work was supported by the Netherlands Science Organisation (NWO) "De Mayerne" project grants 637.000.002 and CHOPII to J. G. H. and M. A. V.

[1] A. E. Martell, R. M. Smith, *Critical Stability Constants. Vol 3*, Plenum Press, New York, **1977**.
[2] J. J. Boon, S. L. Peulve, O. F. van den Brink, M. C. Duursma, D. Rainford in *Early Italian Paintings: Techniques and Analysis*, (Eds.: E. T. Bakkenist, R. Hoppenbrouwers, H. Dubois) Limburg Conservation Institute, Maastricht, **1997**, pp. 35–56.
[3] J. J. Boon, J. Van der Weerd, K. Keune, P. Noble, J. Wadum, "Mechanical and Chemical Changes in Old Master Paintings: Dissolution, Metal Soap Formation and Remineralization Processes in Lead Pigmented Ground/Intermediate Paint Layers of 17th Century Paintings" in *Proceedings of the ICOM-CC 13th Triennial Meeting*, **2002**, pp. 401–406.
[4] P. Noble, A. Van Loon, J. J. Boon, "Chemical Changes in Old Master Paintings II: Darkening Due to Increased Transparency As a Result of Metal Soap Formation" in *ICOM Committee for Conservation 14th Triennial Preprints Den Haag* (Ed.: I. Verger), James and James, London, **2005**, pp. 496–503.
[5] E. S. Claudio, H. A. Godwin, J. S. Magyar, *Prog. Inorg. Chem.* **2003**, *51*, 1–144.
[6] C. Dybowsky, G. Neue, *Prog. Nucl. Magn. Reson. Spectrosc.* **2002**, *41*, 153–170.
[7] F. Fayon, I. Farnan, C. Besada, J. Coutures, D. Massiot, J. P. Coutures, *J. Am. Chem. Soc.* **1997**, *119*, 6837–6843.
[8] Y. Kye, S. Connolly, B. Herreros, G. S. Harbison, *Main Group Met. Chem.* **1999**, *22*, 373–383.
[9] C. E. Holloway, M. Melnik, *Main Group Met. Chem.* **1997**, *20*, 399–495.
[10] F. Rey, J. Antelo, F. Arce, F. Penedo, *Polyhedron* **1990**, *9*, 665–668.
[11] T. Miquel, M. Sanchez, J. Macias, *Can. J. Chem.* **1996**, *74*, 2454–2459.
[12] R. Saxena, C. Chandel, C. Gupta, *Indian J. Chem.* **1989**, *28A*, 625–626.
[13] A. Casale, A. De Robertis, C. De Stefano, A. Gianguzza, G. Patanè, C. Rigano, S. Sammartano, *Thermochim. Acta* **1995**, *255*, 109–141.
[14] H. Yamashita, T. Nozaki, Y. Fukuda, *Bull. Chem. Soc. Jpn.* **1991**, *64*, 697–698.
[15] L. Shimoni-Livny, J. P. Glusker, C. W. Bock, *Inorg. Chem.* **1998**, *37*, 1853–1867.
[16] N. Burford, M. D. Eelman, W. G. LeBlanc, T. S. Cameron, K. N. Robertson, *Chem. Commun.* **2004**, 332–333.
[17] F. H. Allen, *Acta Crystallogr., Sect. B* **2002**, *58*, 380–388.
[18] J. M. Harrowfield, B. W. Skelton, A. H. White, *J. Chem. Soc., Dalton Trans.* **1993**, 2011–2016.
[19] M. Kadarkaraisamy, A. G. Sykes, *Inorg. Chem.* **2006**, *45*, 779–786.
[20] A. Brethon, L. G. Hubert-Pfalzgraf, J. C. Daran, *Dalton Trans.* **2006**, 250–257.
[21] G. D. Fallon, L. Spiccia, B. O. West, Q. Zhang, *Polyhedron* **1997**, *16*, 19–23.
[22] A. Morsali, A. R. Mahjoub, *Helv. Chim. Acta* **2004**, *87*, 2717–2722.
[23] C. A. Steren, R. Calvo, O. E. Piro, B. E. Rivero, *Inorg. Chem.* **1989**, *28*, 1933–1938.
[24] L. Wang, J. Cai, Z.-W. Mao, X.-L. Feng, J.-W. Huang, *Transition Met. Chem.* **2004**, *29*, 411–418.
[25] H. Doucet, T. Ohkuma, K. Murata, T. Yokozawa, M. Kozawa, E. Katayama, A. F. England, T. Ikariya, R. Noyori, *Angew. Chem. Int. Ed.* **1998**, *37*, 1703–1707.
[26] M. Yang, J. Zhou, S. W. Schneller, *Tetrahedron* **2006**, *62*, 1295–1300.
[27] D. Vanderveer, M. L. Colon, X. R. Bu, *Anal. Sci.* **2002**, *18*, 1283–1284.
[28] H. Schmidbaur, I. Bach, D. L. Wilkinson, G. Muller, *Chem. Ber.* **1989**, *122*, 1439–1444.
[29] L. K. Thompson, L. Zhao, Z. Xu, D. O. Miller, W. M. Reiff, *Inorg. Chem.* **2003**, *42*, 128–139.
[30] L. Gasque, S. Bernés, R. Ferrari, C. Barbarín, M. J. Gutierrez-Ponce, G. Mendoza-Díaz, *Polyhedron* **2000**, *19*, 649–653.
[31] K. Umakoshi, Y. Tsuruma, C. E. Oh, A. Takasawa, H. Yasukawa, Y. Sasaki, *Bull. Chem. Soc. Jpn.* **1999**, *72*, 433–440.
[32] M. Bak, J. T. Rasmussen, N. C. Nielsen, *J. Magn. Reson.* **2000**, *147*, 296–330.
[33] U. Haerberlen, *Advances in Magnetic Resonance, Suppl. 1*, Academic Press, New York, **1976**.
[34] M. Mehring, *Principles of High Resolution NMR in Solids*, 2nd ed., Springer Verlag, Berlin, **1983**.
[35] T. Vosegaard, A. Malmendal, N. C. Nielsen, *Chem. Monthly* **2002**, *133*, 1555–1574.
[36] A. Glatfelter, N. Stephenson, S. Bai, C. Dybowski, D. L. Perry, *Analyst* **2006**, *131*, 1207–1209.

[37] A. Glatfelter, C. Dybowski, D. D. Kragten, S. Bai, D. L. Perry, J. Lockard, *Spectrochim. Acta Part A* **2007**, *66*, 1361–1363.
[38] J. Fait, *XSCANS Users Manual*, Siemens Analytical X-ray Instruments, Inc., Madison, WI, USA, **1996**.
[39] G. M. Sheldrick, *SHELX97 Users Manual*, University of Göttingen, Göttingen, Germany, **1997**.
[40] G. M. Sheldrick, *SHELXTL-plus, release 5.10*, Siemens Analytical X-ray Instruments Inc. Madison, WI, USA, **1998**.
[41] H. D. Flack, *Acta Crystallogr., Sect. A* **1983**, *39*, 876–881.
Received: May 27, 2008
Published Online: August 26, 2008

